

# X-Ray Spectral Complexity in Quasars

SH. M. Shehata<sup>1\*</sup>

<sup>\*</sup>National Research Institute of Astronomy and Geophysics, Cairo, Helwan, 11421, EGYPT. ORCID: 0000-0003-3427-1733

## ARTICLE INFO

Received: 02 Jun 2025

Revised: 12 Jul 2025

Accepted: 26 Jul 2025

## ABSTRACT

We present a comprehensive multi-wavelength analysis of quasar sample identified by cross-matching the 3XMM-DR7 X-ray catalog with the SDSS-DR12 optical catalog. To obtain X-ray luminosities, we modeled the spectra of all sources while accounting for soft excess and absorption, and then computed the absorbed luminosities for the full sample. For a subset of 41 quasars with redshifts  $z < 0.5$ , we calculated K-corrected rest-frame optical luminosities using SDSS  $r$ -band magnitudes. We found a statistically significant linear correlation between X-ray and optical luminosities  $\log L_{\text{opt}} = (1.10 \pm 0.07)\log L_X + (-37.55 \pm 3.05)$  with a strong coefficient of determination ( $R^2 = 0.55$ ) and a highly significant p-value ( $p < 10^{-7}$ ). This result supports the disk-corona coupling model in active galactic nuclei, wherein optical/UV photons from the accretion disk are Compton upscattered into the X-ray regime by a hot corona.

**Keyword:** X-ray, Quasars

## 1 INTRODUCTION

Quasars, the most luminous sources powered by the accretion of matter onto supermassive black holes (SMBHs) residing at the centers of galaxies [1, 2]. Their prodigious energy output spans the entire electromagnetic spectrum, from radio to gamma rays, rendering them invaluable probes for multi-wavelength astrophysical investigations [3]. A significant fraction, typically 1–10%, of a quasar's total bolometric luminosity is channeled into the X-ray band, a component widely attributed to inverse Compton scattering of ultraviolet (UV) and optical photons originating from the accretion disk by a surrounding hot, optically thin corona [4, 5, 7]. The intricate interplay between different emission bands, particularly the optical and X-ray regimes, offers a crucial diagnostic for unraveling the complex structure and underlying physics of the quasar central engine. Optical emission primarily arises from the geometrically thin, optically thick accretion disk, while the X-rays are generated within the hot, Comptonizing corona. Consequently, elucidating the relationship between these two distinct emission components provides profound insights into disk-corona interactions, the mechanisms of accretion, and the energetic feedback processes that influence galaxy evolution [26, 8]. Intriguingly, observational evidence often suggests an inverse correlation, where quasars exhibiting strong optical luminosity tend to display comparatively lower X-ray emission, and vice versa, hinting at a nuanced balance in energy distribution and transfer efficiency across these components. A comprehensive exploration of such intricate trends necessitates large, statistically robust samples and precise, synchronized multi-wavelength measurements. Recent advancements in wide-field astronomical surveys have revolutionized our ability to conduct such investigations. Catalogs such as the 3XMM-DR7 from *XMM-Newton* [9] and the Sloan Digital Sky Survey (SDSS-DR12) [10] provide unprecedented access to high-quality X-ray and optical data, respectively. The cross-matching of these extensive datasets facilitates the discovery of previously uncharacterized sources and enables large-scale statistical studies of quasar properties across diverse cosmic epochs. This synergistic approach is indispensable for understanding the multi-wavelength behavior of quasars and for identifying subtle yet critical phenomena, such as spectral soft X-ray excess and additional emission

<sup>1</sup> National Research Institute of Astronomy and Geophysics, Cairo, Helwan, 11421, EGYPT. ORCID: 0000-0003-3427-1733

component typically observed below  $\sim 2$  keV and intrinsic absorption. Both soft excess and absorption can significantly modify the observed X-ray spectrum, potentially leading to biased characterizations if not meticulously accounted for. For instance, an uncorrected soft excess can artificially flatten the X-ray spectrum, resulting in poor fits with simplistic power-law models. Therefore, rigorous testing for and accurate modeling of these spectral components are paramount for a precise determination of intrinsic quasar properties.

In this context, our work aims to contribute significantly to the ongoing efforts to unravel the complexities of quasar physics. By meticulously analyzing a substantial sample of 544 quasars, leveraging the rich multiwavelength data from 3XMM-DR7 and SDSS-DR12, we seek to provide a robust characterization of their X-ray and optical luminosities. Crucially, our methodology emphasizes a rigorous treatment of spectral complexities, including soft X-ray excess and intrinsic absorption, to ensure the derivation of accurate intrinsic parameters. This detailed approach will not only refine our understanding of the fundamental relationship between optical and X-ray emission in quasars but also shed light on the physical processes governing accretion, energy transfer, and feedback in these extreme cosmic environments.

## 2 DATA ANALYSIS

### 2.1 Catalogs and Data Selection

The X-ray catalog XMM-DR7 for XMM fields provides a comprehensive list of new objects, each annotated with various quality and technical flags. It contains 499,266 unique X-ray sources, classified into star clusters, globular clusters, gaseous nebulae, and spiral nebulae. From the 3XMM-DR7 catalog, consisting of 727,790 X-ray detections, we identified galaxy clusters among point-like sources, including stars and quasars, by selecting sources with EP-EXTENT = zero, estimating around 660,452 point-like sources with EPIC extent radius less than 6 arcseconds. To improve sample quality, sources affected by high background noise or flagged with values greater than 1, 2, or 3, were discarded, leaving 349,741 sources. Further improvement involved removing repeated detections and focusing on sources with counts exceeding 600, resulting in a final set of 14,323 high-quality point sources. Similarly, the Sloan Digital Sky Survey (SDSS) is a vast spectroscopic and photometric survey covering approximately 14,555 square degrees. The SDSS quasar catalog mainly comprises objects with measured positions and properties such as magnitudes across five photometric bands (u, g, r, i, z). The final sample of SDSS-DR12 catalog after excluding blazars and selecting objects flagged with SDSS-MORPHO = 0 yielded 244,475 quasars. Crossmatching the cleaned X-ray sample with SDSS-DR12 final sample using a positional search radius of 5 arcseconds and tools like TOPCAT for visualization and editing, we identified 593 mutual sources present in both catalogs, comprising both newly discovered sources and previously known SDSS-DR7 quasars. After excluding overlapping sources in each X-ray observation and applying stricter quality criteria such as background filtering the final sample consisted of 544 X-ray and optical cross-identified quasars.

### 2.2 XMM Reduction

The XMM-Newton observatory is equipped with three X-ray telescopes, each housing an X-ray CCD detector as part of the European Photon Imaging Camera (EPIC) system. EPIC comprises three cameras: PN, MOS1, and MOS2 [13], each providing a spatial resolution of approximately 1.5 arcseconds across the field of view. In this study, all EPIC-pn observations for all the sample. The raw observational data were processed with the XMM-Newton Science Analysis System (SAS), utilizing the latest calibration files. Initial event correction was performed using the meta-task epcchain. Background flares—often occurring at the start and end of exposures—were identified and excluded to ensure data quality. Instrument response matrices were generated and applied; ancillary response files (ARFs) were created using the SAS task arfgen, and redistribution matrix files (RMFs) were produced with rmfgen. Finally, the extracted X-ray spectra were grouped using the HEASARC tool grppha for subsequent analysis.

### 2.3 Spectral Fitting

The physical properties of these quasars were estimated through X-ray spectral fitting of available XMM-Newton observations. To ensure data quality, observations recorded in timing mode or affected by incomplete imaging from single-chip data were excluded.

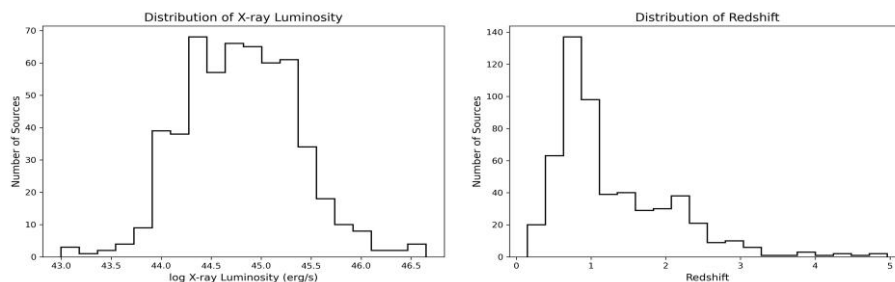


**Figure 1: Left: Histogram showing the distribution of X-ray luminosities (0.5–10 keV) for the 544 quasars in the sample, expressed as  $\log L_X$  in  $\text{erg s}^{-1}$ . The luminosities span a wide range, with the majority of sources concentrated between  $10^{44}$  and  $10^{45} \text{ erg s}^{-1}$ . Right: Histogram of redshift distribution for the same sample, ranging from  $z = 0.148$  to  $z = 4.96$ . The distribution peaks at low redshift ( $z < 1$ ), with a gradual decline toward higher redshifts, reflecting the observational sensitivity and selection effects of the combined XMM-Newton and SDSS surveys.**

Spectral fitting was conducted using XSPEC, developed by NASA's HEASARC, focusing on the 0.3–10 keV energy band. Periods of high background radiation were excluded, and all spectra were fitted employing the Cash statistic [11] along with the TBABS model to account for Galactic absorption. From each fit, we derived the X-ray luminosity (0.5–10 keV) in the same band, expressed in  $\text{erg s}^{-1}$ . These measurements were obtained for 544 spectra using the EPIC-pn camera onboard XMM-Newton. The X-ray spectra of our quasar sample are well described by a redshifted power-law model (zpowerlaw), with an average photon index of approximately  $\Gamma \sim 1.84$ . The sample spans X-ray luminosities from  $L_X = 9.93 \times 10^{42}$  to  $4.46 \times 10^{46} \text{ erg s}^{-1}$  and covers a redshift range from  $z = 0.148$  to 4.96.

## 3 SPECTRAL EFFECTS AND PHYSICAL CHARACTERISTICS OF THE SAMPLE

Good observations in multi-wavelength bands support statistical study to understand physical processes that occur in quasars. In fact, correlations between physical parameters have been extensively investigated. In this section we will check all the properties that can affect our sample to be sure that we obtain the best X-ray results.

### 3.1 Effect of Soft Excess

In this section, we examine the presence and impact of soft X-ray excess in our quasar sample. We selected spectra with reduced C-statistics greater than 1.5, indicating potential deviations from a simple power-law model.

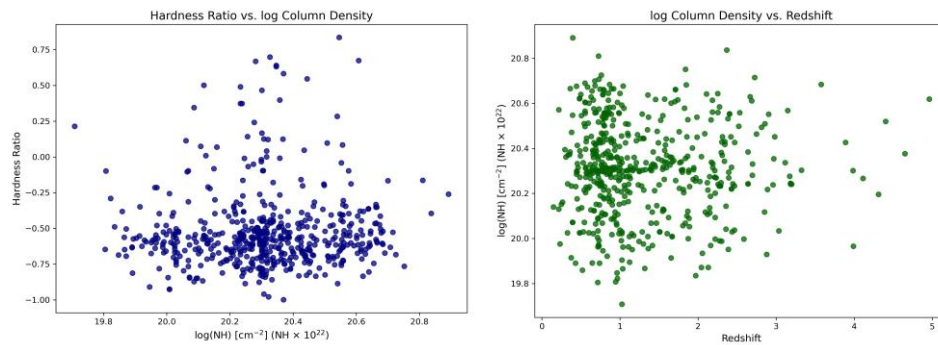


**Figure 2: Left: Scatter plot showing the relationship between hardness ratio and logarithmic hydrogen column density ( $\log N_H$  in  $\text{cm}^{-2}$ ) for the quasar sample. Most sources cluster around negative hardness ratios, consistent with low X-ray obscuration, while a small number show higher values possibly indicating moderate absorption. Right: Scatter plot of hydrogen column density versus redshift. The absence of a clear trend suggests no significant dependence of column density on redshift, in agreement with previous results that intrinsic absorption is relatively uniform across cosmic time for quasars.**

To these spectra, we added a blackbody (BB) component to the redshifted power-law model, fixing the blackbody temperature at 0.1 keV, following the methodology of [19], [18], and [20]. We got improved in almost 80 % of the spectra with reduced c-stat decrease, this improvement appear in 121 source. This is consistent with the detection of soft excess emission a well-known feature in AGNs attributed to thermal radiation from the innermost regions of the accretion disk.

Soft excess typically appears as a significant rise in the X-ray spectrum below 2.0–3.0 keV [17]. Its origin is generally linked to thermal emission from the hot inner accretion disk [16]. The effective temperature of this component is lower in the soft X-ray band due to the electron population responsible for inverse Compton scattering, with typical values around 0.1 keV.

### 3.1.1 Hardness Ratio and absorbed Sources

The hardness ratio (HR) is a useful diagnostic for estimating the degree of X-ray obscuration in quasars and provides a good signal-to-noise ratio (S/N) when measured across both soft and hard X-ray bands. It can only be calculated consistently for observations obtained from the same instrument. The HR is defined as

$$\text{HardnessRatio} = \frac{CR_{2.0-10.0} - CR_{0.5-2.0}}{CR_{0.5-2.0} + CR_{2.0-10.0}} \quad (1)$$

where  $CR_{2.0-10.0}$  is the count rate in the hard X-ray band (2.0–10.0 keV), and  $CR_{0.5-2.0}$  is the count rate in the soft band (0.5–2.0 keV) [12]. The HR ranges from  $-1$  to  $+1$ , where more negative values indicate lower absorption and softer spectra.

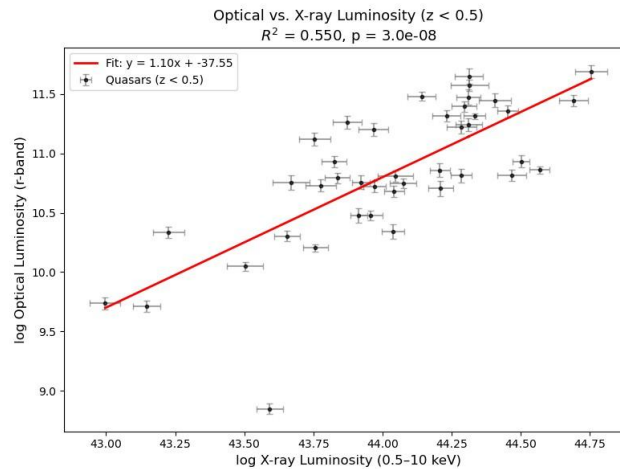


**Figure 3: Scatter plot showing the correlation between log optical luminosity (r-band) and log X-ray luminosity (0.5–10 keV) for quasars with  $z < 0.5$ . The red line indicates the best-fit linear regression.**

All HR values were calculated from data collected with the EPICpn camera onboard *XMM-Newton*. The average hardness ratio for our sample of 544 quasars is  $-0.51$ , suggesting that most of the sources are only mildly obscured.

Figure 2 (left panel) shows the relationship between the hardness ratio and the logarithmic hydrogen column density ( $N_H$ ). The distribution indicates low absorption for most quasars, with a small number exhibiting higher  $N_H$  values. In Figure 2 (right panel), we plot the correlation between  $N_H$  and redshift. No significant trend is found, confirming previous results that absorption and redshift are largely independent for quasars [15].

The complexity of quasar spectra means that accurate absorption measurements can be affected by multiple components. If features such as soft excess or scattered nuclear emission are not considered, the resulting absorption estimates may be inaccurate [14]. To better classify sources, we applied an additional absorption model (ZTBABS) to spectra that did not improve after adding BB. We found that 40 quasars showed significant improvement in fit after including this intrinsic absorption component. Interestingly, in many of these sources, the derived column densities were smaller than the Galactic values, suggesting the presence of warm ionized absorbers or partial covering effects rather than cold neutral gas.

#### 4 OPTICAL AND X-RAY LUMINOSITY CORRELATION

To investigate the relationship between the accretion disk and X-ray corona, we analyze the correlation between optical and X-ray luminosities of quasars at redshifts  $z < 0.5$ , where k-corrections can be computed reliably. First, k-corrections were obtained using the TOPCAT tool, assuming a power-law continuum with index  $\alpha = -0.5$ . These k-corrections were derived using SDSS DR12 r-band photometry. From the absolute magnitudes, we then estimated the optical luminosities. The absolute magnitudes were calculated via:

$$M_r = m_r - 5\log_{10}(D_L) + 5 - K(z), \quad (2)$$

where  $D_L$  is the luminosity distance computed using a flat  $\Lambda$ CDM cosmology ( $H_0 = 70 \text{ km s}^{-1} \text{ Mpc}^{-1}$ ,  $\Omega_M = 0.3$ ,  $\Omega_\Lambda = 0.7$ ), and  $K(z)$  is the k-correction.

We estimate optical luminosities for 41 quasars with  $z < 0.5$ . For this subset, we find a statistically significant correlation between log X-ray luminosity and log optical luminosity. A linear regression yields:

$$\log L_{\text{opt}} = (1.10 \pm 0.07)\log L_X + (-37.55 \pm 3.05), \quad (3)$$



with a coefficient of determination  $R^2 = 0.55$  and  $p$ -value  $< 10^{-7}$ . This suggests a moderate-to-strong connection between the optical and X-ray emitting regions, consistent with disk-corona models. Figure 3 shows the correlation between optical and X-ray luminosity of the quasar sample.

## 5DISCUSSION

In this study, we analyzed a multi-wavelength sample of 544 quasars selected through cross-matching the X-ray catalog 3XMM-DR7 and the optical catalog SDSS-DR12. This allowed us to explore the physical properties of quasars across a broad redshift range ( $z = 0.148$  to  $4.96$ ) and investigate the connection between their X-ray and optical emission.

We began by estimating the X-ray luminosities of all sources, but before finalizing these values, we examined two major spectral features that could influence the intrinsic emission: soft excess and X-ray absorption. First, we applied a blackbody (BB) component with a fixed temperature of  $0.1$  keV to the spectra with reduced  $\chi^2$ -statistics greater than  $1.5$ . This improved the fit in 121 quasars, indicating the presence of a soft X-ray excess which is a feature commonly observed in AGNs and typically attributed to thermal emission from the innermost regions of the accretion disk or Comptonization of disk photons [23, 24]. The presence of this soft excess in a significant fraction of our sample highlights the complex interaction between the accretion flow and the corona. For the remaining spectra that did not improve with a soft excess component, we tested for intrinsic absorption by adding the ZTBABS model.

We identified 40 quasars with improved fit quality, classifying them as absorbed sources. Interestingly, the estimated column densities for many of these quasars were below the Galactic values, suggesting that absorption may originate from a mildly ionized material or partial covering, rather than a dense, neutral gas [25]. Our hardness ratio analysis, which yielded an average value of  $HR = -0.51$ , further supports this picture, indicating that most sources in our sample are only weakly obscured.

The derived average photon index from our X-ray spectral fitting is

$\Gamma \approx 1.84 \pm 0.3$ , which is in strong agreement with previous studies of AGN power-law spectra [26, 27]. This value supports the widely accepted model in which X-ray emission originates from inverse Compton scattering of optical/UV photons from the accretion disk by hot electrons in a surrounding corona [4]. The broad distribution of X-ray luminosities in our sample (from  $9.93 \times 10^{42}$  to  $4.46 \times 10^{46}$  erg s $^{-1}$ ) confirms that our results reflect the diverse nature of the quasar population across different epochs.

After correcting for both soft excess and absorption, we estimated the absorbed X-ray luminosities. We then moved to the optical side of the analysis, where we focused on 41 quasars with redshifts  $z < 0.5$  to ensure accurate  $k$ -correction. We calculated their rest-frame optical luminosities based on SDSS  $r$ -band magnitudes and performed a correlation analysis between their optical and X-ray luminosities.

Our regression analysis revealed a statistically significant linear correlation:

$\log L_{\text{opt}} = (1.10 \pm 0.07)\log L_X + (-37.55 \pm 3.05)$ , (4) with  $R^2 = 0.55$  and a  $p$ -value  $< 10^{-7}$ . This result provides strong evidence for a moderate-to-strong connection between the optical and X-ray emitting regions in quasars. It is consistent with the disk-corona model, where X-rays are produced through inverse Compton upscattering of disk photons by the hot corona. The correlation also hints at more complex physical processes such as radiative feedback, inclination effects, or reprocessing, which can affect the observed slope and scatter [3].

Several studies have investigated the correlation between X-ray and optical luminosities in quasars, Kriss [21] found that for radio-quiet quasars, the X-ray and optical luminosities follow a significantly nonlinear relation, with weak redshift dependence. This suggests a systematic change in the X-ray continuum with increasing luminosity, implying either a flattening of the X-ray continuum or a decrease in its overall normalization relative to the optical. Lusso et al. [22] also found a highly significant correlation between X-ray and optical luminosity in a sample of X-ray selected type 1 AGN, consistent with previous investigations. Their work showed that the ratio between X-ray and optical flux decreases with increasing Eddington ratio. These results collectively strengthen the interpretation of our observed correlation within the framework of the disk-corona model, emphasizing the fundamental link between the optical and X-ray emission in quasars.

## 6 CONCLUSION

In this study, we presented a detailed X-ray investigation of 544 quasars jointly identified in the 3XMM-DR7 X-ray catalog and the SDSS-DR12 optical catalog. Our key result include the following

**Spectral Modeling** The X-ray spectra are well-described by a redshifted power-law with an average photon index  $\approx 1.84$ , indicative of inverse Compton scattering in a hot corona.

**Soft Excess Detection:** Approximately 121 quasars exhibit soft excess emission, consistent with thermal radiation from the innermost regions of the accretion disk.

**Absorption Effects:** Hardness ratio analysis reveals low overall absorption, with only 40 quasars showing signs of significant intrinsic absorption based on spectral modeling.

**X-ray–Optical Correlation** For a subsample of low-redshift quasars ( $z$  less than 0.5), we observe a statistically significant correlation between X-ray and optical luminosity, supporting the disk–corona connection. Our analysis demonstrates the value of combining large-area optical and X-ray surveys to statistically probe the physical mechanisms of quasar emission. The presence of soft excess and mild absorption in many sources points to the diversity of accretion and reprocessing environments in AGNs.

## REFERENCES

- [1] Rees, M. J. (1984). "Black holes, gravitational waves and cosmology: An introduction to current research." In *General Relativity and Gravitation* (pp. 207-221). Springer, Boston, MA.
- [2] Kormendy, J., & Ho, L. C. (2013). "Co-evolution (Or Not) of Supermassive Black Holes and Host Galaxies." *Annual Review of Astronomy and Astrophysics*, 51, 511-653.
- [3] Elvis, M., Wilkes, B. J., McDowell, J. C., et al. (1994). "Atlas of quasar energy distributions." *The Astrophysical Journal Supplement Series*, 95, 1-68.
- [4] Shakura, N. I., & Sunyaev, R. A. (1973). "Black holes in binary systems. Observational appearance." *Astronomy and Astrophysics*, 24, 337-355.
- [5] Galeev, A. A., Rosner, R., & Vaiana, G. S. (1979). "Radiation from the accretion disk in active galactic nuclei." *The Astrophysical Journal*, 229, 318-326.
- [6] Shemmer, O., Brandt, W. N., Netzer, H., et al. (2005). "The X-ray properties of high-redshift quasars." *The Astrophysical Journal*, 630, 689-703.
- [7] Haardt, F., & Maraschi, L. (1991). "A two-phase model for the X-ray emission from Seyfert galaxies." *The Astrophysical Journal*, 380, L51-L54.
- [8] Merloni, A., Heinz, S., & Di Matteo, T. (2003). "A fundamental plane of black hole accretion." *Monthly Notices of the Royal Astronomical Society*, 345, 1057-1076.
- [9] Rosen, S. R., Webb, N. A., Watson, M. G., et al. (2016). "The XMM-Newton serendipitous survey: The 3XMM-DR7 catalog." *Astronomy & Astrophysics*, 590, A1.
- [10] Paris, I., Petitjean, P., Ross, N. P., et al. (2017). "The Sloan Digital Sky Survey Quasar Catalog: DR12." *Astronomy & Astrophysics*, 597, A103.
- [11] Cash, Webster, *The Astrophysical Journal*, 1979, 228, 939-947 [12] Fotopoulou, S., et al. *Astronomy & Astrophysics* 592 (2016): A5.
- [13] Turner M. et al. 2001, *A&A*, 365, L27.
- [14] Wilkes, Belinda J., et al. *The Astrophysical Journal* 773.1 (2013): 15.
- [15] Giustini, Margherita, Massimo Cappi, & Cristian Vignali. *Astronomy & Astrophysics* 491.2 (2008): 425-434.
- [16] Malkan M., Sargent W., 1982, *ApJ*, 254, 22.
- [17] Comastri, A., Setti, G., Zamorani, G., Elvis, M., Wilkes, B. J., McDowell, J. C., Giommi, P., 1992, *ApJ*, 384, 62
- [18] Singh, K. P. *Bull. Astr. Soc. India* 41 (2013): 137-157.
- [19] Fabian A.C. et al., 2002, *MNRAS*, 335, L1
- [20] Shehata, S. M., Misra, R., Osman, A. M. I., et al. 2021, *Journal of High Energy Astrophysics*, 31, 37. doi:10.1016/j.jheap.2021.04.003
- [21] Kriss, G. A. (1988). "X-ray, optical, and IR luminosity correlations in quasars." NASA Technical Reports Server (NTRS).

- [22] Lusso, E., Comastri, A., Vignali, C., et al. (2010). "The X-ray to optical-UV luminosity ratio of X-ray selected type 1 AGN in XMMCOSMOS." *Astronomy & Astrophysics*, 512, A34.
- [23] Malkan, M. A. (1982). "The ultraviolet excess of quasars: A consequence of accretion disk models." *The Astrophysical Journal*, 268, 582-590.
- [24] Comastri, A., Setti, G., Zamorani, G., et al. (1992). "The X-ray properties of quasars and their implications for the X-ray background." *The Astrophysical Journal*, 384, 62-72.
- [25] Wilkes, B. J., Kuraszkiewicz, J., Haas, M., et al. (2013). "The X-ray properties of type 2 quasars." *The Astrophysical Journal*, 770, 117.
- [26] Shemmer, O., Brandt, W. N., Netzer, H., et al. (2005). "The X-ray properties of high-redshift quasars." *The Astrophysical Journal*, 630, 689-703.
- [27] Piconcelli, A., Jimenez-Bailon, E., Guainazzi, M., et al. (2005). "The X-ray properties of a sample of high-redshift quasars." *Astronomy & Astrophysics*, 432, 15-26.